DOI: 10.1002/cbic.200500546

Directed Evolution of an Esterase from *Pseudomonas fluorescens* Yields a Mutant with Excellent Enantioselectivity and Activity for the Kinetic Resolution of a Chiral Building Block

Marlen Schmidt,[a] Daniel Hasenpusch,[b] Markus Kähler,[c] Ulrike Kirchner,[c] Kerstin Wiggenhorn,[c] Walter Langel,[b] and Uwe T. Bornscheuer*[a]

A triple mutant of an esterase from Pseudomonas fluorescens *(PFE) that was created by directed evolution exhibited high enantioselectivity (E = 89) in a kinetic resolution and yielded the building block (S)-but-3-yn-2-ol. Surprisingly, a mutation close to the active site caused the formation of inclusion bodies, but remote mutations were found to be responsible for the high selectivity. Back mutations gave a variant (double mutant PFE Ile76Val/Val175Ala) that showed excellent selectivity (E = 96) and activity (20 min for 50% conversion, which corresponds to 1.25 U per mg of protein).*

Introduction

Directed evolution has emerged in the past decade as the most powerful method for improving biocatalysts.[1] For instance, the enantioselectivity of a D-hydantoinase could be reversed, thus leading to a substantially improved process for the synthesis of optically pure L-amino acids.[2] Reetz and Jaeger were able to increase the enantioselectivity of a lipase from *Pseudomonas aeruginosa* towards a chiral carboxylic acid (2-methyl decanoate), initially from $E = 1.1$ (wild-type or WT) to $E = 11$.[3] Using a combination of a broad range of molecular biology methods they were finally able to identify a variant with practically useful selectivity ($E = 51$).[4] Similarly, we have been able to increase the enantioselectivity of an esterase from *Pseudomonas fluorescens* (PFE) towards 3-phenylbutyric acid from $E = 3.5$ to $E = 12$ by combining error-prone PCR (epPCR) with saturation mutagenesis.[5]

Successful directed-evolution experiments depend on several aspects. The identification of desired variants that exhibit an increased enantioselectivity strongly depends on the high-throughput screening (HTS) method used—the selectivity determined with a surrogate substrate (i.e., a *p*-nitrophenyl ester) can differ significantly from the true substrate (i.e., a methyl ester), which can lead to false-positive variants. In addition, it is assumed that the random introduction of mutations does not significantly affect other properties of the biocatalyst and its production in the microbial host. Another aspect is the location of productive mutations. Directed-evolution experiments have often led to variants in which effective mutations were far from the active-site region, although they affected substrate specificity or enantioselectivity. Consequently, the question of whether closer mutations are better has been already addressed in the literature.[6]

The hydrolase-catalyzed resolution of the acetate of **1a** (Scheme 1) is very challenging as this secondary alcohol has only small differences in the size of its substituents. In accordance with "Kazlauskas' rule",[7] it is converted by lipases or esterases only with low to modest *E* values.

The (*R*)-alcohol can be used for the synthesis of (−)-akolactone A a cyctotoxic butenolide,[8] pancrastatin an antitumour alkaloid,[9] chiral cyclopropane-based ligands[10] and for the large-scale production of (*R*)-benzyl 4-hydroxylpent-2-ynoate.[11] Both pure enantiomers of **1a** have been employed in the preparation of enantio- and diastereomerically pure allylboronic ester by Johnson rearrangement, which led to enantiopure homoallyl alcohols.[12] Other examples include the synthesis of 3-bromopyrrolines from α-amino allenes,[13] optically active bicyclic ligands used for the synthesis of HIV protease inhibitors[14] or key intermediates of $\alpha_v\beta_3$ antagonist (useful for the treatment of osteoporosis).[15] One example for an application of the (*S*)-alcohol is the preparation of chiral cyclic carbonates.[16]

Previously, we investigated more than 100 hydrolases for the kinetic resolution of **1b**[17] and the best enzyme was the ester-

[a] *Dr. M. Schmidt, Prof. Dr. U. T. Bornscheuer*
Institute of Biochemistry, Department of Biotechnology & Enzyme Catalysis
Greifswald University, Soldmannstrasse 16, 17487 Greifswald (Germany)
Fax: (+49) 3834-86-80066
E-mail: uwe.bornscheuer@uni-greifswald.de

[b] *D. Hasenpusch, Prof. Dr. W. Langel*
Institute of Biochemistry, Department of Biophysical Chemistry
Greifswald University, Greifswald (Germany)

[c] *Dr. M. Kähler, Dr. U. Kirchner, K. Wiggenhorn*
Dr. Rieks Healthcare GmbH
Deichstrasse 25a, 25436 Uetersen (Germany)

ase from *P. fluorescens* expressed in *E. coli*.[18] However, detailed analysis of the reaction time course revealed that the enantioselectivity dropped considerably during hydrolysis of the acetate and complete conversion was observed (Figure 1 A; Table 1), which led to racemic alcohol **1 a**. A similar effect was described in a patent for an esterase from *Burkholderia glumae* (previously designated *Pseudomonas glumae)*.[19] In the hydrolysis of the corresponding butyrate, the initial value was $E \sim 30$, but also dropped at higher conversion which made a high-yield resolution impractical. Only Nakamura and co-workers have reported acceptable enantioselectivity, but the small-scale resolution suffered considerably from the use of large amounts of lipase Amano AH and very long reaction times (2 days).[20] The alternative asymmetric enzymatic reduction of the ketone was hampered by the very low enantiomeric excess, as shown for a NADPH-dependent alcohol dehydrogenase from *Lactobacillus brevis*, which afforded the (*R*)-alcohol with 60% *ee* or a NADH-dependent *Candida parapsilosis* carbonyl reductase that yielded the (*S*)-alcohol with 49% *ee*.[21] In addition, but-3-yn-2-one is rather unstable and has high risk of thermal decomposition, which would restrict its large-scale reduction even if a highly selective reductase were available.

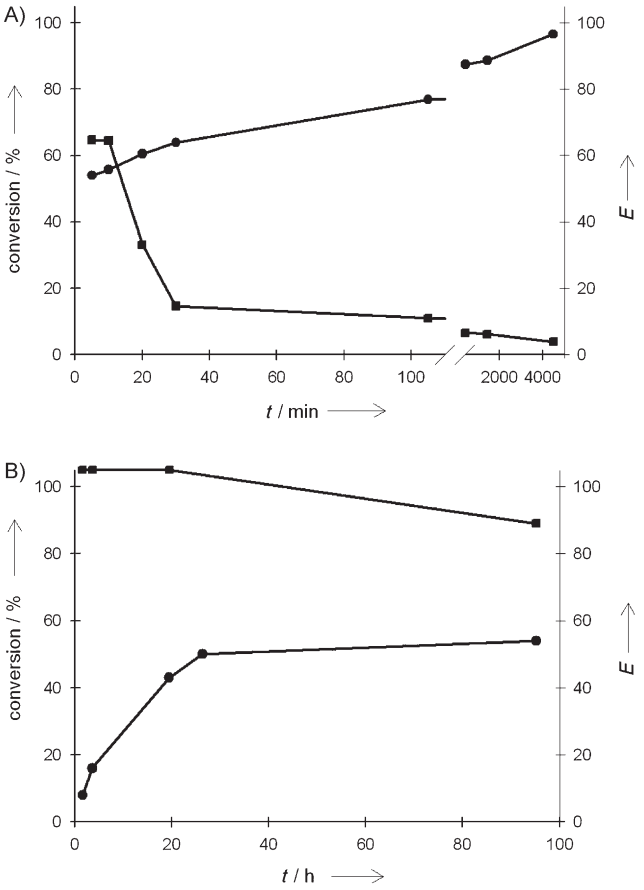

Figure 1. Hydrolysis of **1 b** with A) wild-type PFE, and B) the PFE triple mutant (Ile76Val/Gly98Ala/Val175Ala); (●) conversion; (■) enantioselectivity.

In this work, we used methods of directed evolution to improve the enantioselectivity of an esterase by using the secondary alcohol *rac*-but-3-yn-2-ol as target compound (**1 a**; Scheme 1). As detailed below, the number and positions of amino-acid substitutions gave rather unexpected results.

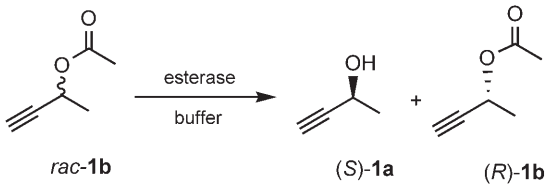

Scheme 1. Principle of esterase-catalyzed kinetic resolution.

Results and Discussion

To create an enantioselective variant for resolving **1 b**, epPCR libraries with a mutation rate of one to two mutations per gene of PFE were created, followed by HTS by using the "acetic-acid assay" previously developed in our laboratory.[22] Acetic acid released in the esterase-catalyzed hydrolysis of acetate **1 b** was stoichiometrically converted in an enzyme-cascade reaction

Table 1. Specific activities of wild-type PFE and its variants towards *p*NPA, their *E* values at 50% conversion and their enantioselectivity after prolonged reaction times (E_{max}).

Name	PFE variant	Activity [U per mg protein] lyophilisate	IB[a]	$E \sim 50\%$[b]	*t* [min]	E_{max}[c]	*t* [min]
WT	wild-type	77	–	63	5	3 (96%)	1440
V2A	Ile76Val/Gly98Ala/Val175Ala	0.006	+	89	5700	89 (54%)	5700
2A	Gly98Ala/Val175Ala	0.2	+	>100[d]	180	>100 (40%)	180
VA_1	Ile76Val/Gly98Ala	0.6	+	80[e]	10	80 (25%)	10
A_1	Gly98Ala	9	+	>100	5	90 (57%)	1500
VEA_2	Ile76Val/Asp99Glu/Val175Ala	37	–	92	420	92 (53%)	420
V	Ile76Val	49	–	>100	1	16 (83%)	1500
VA_2	Ile76Val/Val175Ala	57	–	96	20	96 (53%)	20
A_2	Val175Ala	67	–	>100	1	26 (74%)	1500

[a] IB: inclusion body; [b] calculated at 50% conversion; [c] calculated at maximal conversion given in brackets (%); [d] calculated at 40% conversion; [e] calculated at 25% conversion.

into NADH, which was quantified spectrophotometrically at 340 nm. As enantiopure (*R*)- and (*S*)-acetates were used in separate wells of a microtiter plate, the apparent enantioselectivity (E_{app}) of each esterase variant could be determined from these initial rate measurements. The *E* values were then confirmed by kinetic resolution after shake-flask production of positive variants in small-scale experiments by GC analysis (E_{true}). After screening ~7000 mutants, a PFE mutant was identified that exhibited an $E_{true}=89$ at 54% conversion. Unfortunately, the reaction time was extremely long (>24 h; Figure 1B) compared to only a few minutes required for similar conversion values when using the wild-type PFE (Figure 1A).

Sequencing of this variant identified three point mutations (Ile76Val/Gly98Ala/Val175Ala). Surprisingly, cell fractionation and analysis of the pellet by SDS-PAGE showed that this triple mutant—in contrast to the WT—was produced as inclusion bodies (IBs) and only a minor fraction of soluble protein was formed. This had a specific activity of only 0.006 U per mg protein ($V_{max}/K_M=5.3\times10^{-5}$ min^{-1}) compared to 77 U per mg protein ($V_{max}/K_M=0.57$ min^{-1}) for the wild-type PFE when using *p*-nitrophenyl acetate (*p*NPA) as assay substance. IB formation could be slightly decreased by incubating host cells at 25 °C, which yielded a specific activity of 0.5 U per mg protein.

To locate the mutations, a model of the triple mutant was created based on the known 3D structure of PFE[23] (PDB ID: 1VA4; Figure 2). From this structure, it was initially assumed that the Gly98Ala mutation close to the catalytic triad of the esterase (Ser94, His251, Asp222) led to the substantial increase in enantioselectivity ("closer is better"),[6] and that the other two remote mutations (Ile76Val, Val175Ala) were responsible for the formation of IBs.

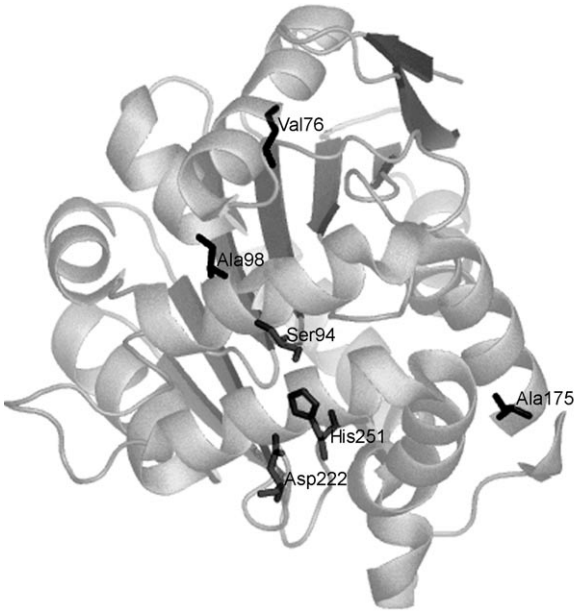

Figure 2. 3D homology model of PFE. The catalytic triad is shown in grey (Ser94, His 251, Asp222), mutation sites are highlighted in black (Val76, Ala98 and Ala175). The model was created by using PyMOL and amino-acid exchanges were introduced with the "Wizard/Mutagenesis" feature (http://pymol.sourceforge.net).

To verify this assumption, all corresponding double and single mutants were created by QuikChange site-directed mutagenesis (Table 1). Beside the planned variants, an additional mutation was found at position 99 (Asp99Glu).

Four variants (VEA_2, V, VA_2 and A_2) that lacked the Gly98Ala mutation exhibited specific activities similar to the WT enzyme without IB formation. It is worth noting that variant VEA_2 (Ile76Val/Asp99Glu/Val175Ala) formed no IBs (compared to V2A) and had a specific activity similar to the WT. From this we concluded that the Gly98Ala mutation (A_1) next to the catalytic triad must be responsible for IB formation.

To gain a deeper insight into the structural reasons for our experimental findings a molecular-dynamic simulation of both enzyme variants, wild-type PFE and the triple mutant V2A, were performed with an AMBER94 force field implemented in the AMBER7 package, which included the TIP3P model for water. An alignment of both resulting structures was performed with PyMOL (http://pymol.sourceforge.net). In the triple mutant V2A a helix extended by one loop was identified at position 98 (Figure 3). Here, the helix breaker, glycine,[24] was

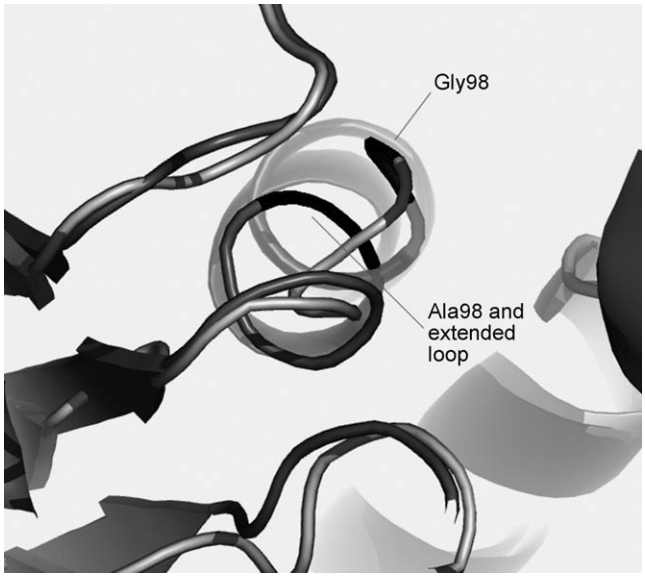

Figure 3. Alignment of WT (light grey, Gly98 labelled) and triple mutant V2A (dark grey, Ala98 labelled); the extended loop of the helix is highlighted.

replaced by the helix creator, alanine, at the end of the α-helix. This new conformation appears to destroy the original tertiary structure and might result in the formation of IBs. No significant alterations at the other two mutated positions were observed.

Next, the enantioselectivity of all variants was investigated by small-scale resolutions and we were pleased to find, that two mutants exhibited satisfying activity and also enantioselectivity in the resolution of **1b** without further conversion and reduction in *E* values: the double mutant VA_2 (Ile76Val/Val175Ala) with $E=96$ (53% conversion, 20 min, 1.25 U per mg protein) and a specific activity towards the standard substrate *p*NPA of 57 U per mg protein ($V_{max}/K_M=0.51$ min^{-1}), and VEA_2

(Ile76Val/Asp99Glu/Val175Ala) with $E=92$ (53% conversion, 7 h, 0.06 U per mg protein) and a specific activity of 37 U per mg protein ($V_{max}/K_M=0.31\ min^{-1}$). Both variants have the same temperature stability and pH optimum as wild-type PFE (data not shown).

Thus, by using directed evolution and subsequent site-directed mutagenesis, we were able to create several esterase variants that showed excellent enantioselectivity and kinetics in the resolution of the acetate of but-3-yn-2-ol to yield the (*S*)-enantiomer. Due to their high selectivity and activity with these variants, the (*R*)-enantiomer was also available from the remaining acetate.

Beside the creation of a biocatalyst that is useful for efficient kinetic resolution, this study has also shown that a mutation close to the active site can have a substantial impact on protein folding. This aspect has not been described so far in the literature and should be considered further in protein engineering, especially when using directed-evolution methods. In addition, mutations near the active site do not necessarily lead to altered enantioselectivity and in this case remote mutations were shown to be most effective in creating a highly enantioselective enzyme.

Furthermore, this is the first example of the successful creation of an esterase with substantially improved enantioselectivity towards secondary alcohols, obtained by using methods of directed evolution.

Experimental Section

General: All chemicals were purchased from Fluka (Buchs, Switzerland), Sigma (Steinheim, Germany) and Merck (Darmstadt, Germany) unless stated otherwise. Restriction enzymes, ligase, DNAseI and polymerases were obtained from Promega (Madison, WI, USA) and New England BioLabs GmbH (Beverly, MA, USA). MWG-Biotech (Ebersberg, Germany) provided primers and performed the sequencing experiments.

Bacterial strains, plasmid, growth conditions and protein analysis: *E. coli* DH5α or JM109 were used as hosts for transformation of plasmid DNA. The strains were grown at 37 °C in Luria–Bertani (LB) liquid media or on LB agar plates supplemented with ampicillin (100 μg mL^{-1}).[25] The vector pJOE2792.1 with a rhamnose-inducible promoter was used for expression of PFE. Esterase production was induced upon addition of rhamnose (final concentration 0.2%, *v*/*v*) and the culture was continued for 5 h. Cells were collected by centrifugation (15 min, 4 °C, 3939 *g*) and washed twice with sodium phosphate buffer (10 mM, pH 7.4, 4 °C). Cells were disrupted by sonication on ice for 5 min at 50% pulse and centrifuged to separate soluble from insoluble fractions, the latter contained the IBs. The supernatant was lyophilized and stored at 4 °C. Protein content was determined by using Bradford reagent with bovine serum albumin as standard.

Esterase activity was determined spectrophotometrically by hydrolysis of *p*NPA (10 mM in DMSO) in sodium phosphate buffer (10 mM, pH 7.4). Released *p*-nitrophenol was quantified at 410 nm ($\varepsilon=15\times10^3\ M^{-1}cm^{-1}$). One unit (U) of activity was defined as the amount of enzyme that released 1 μmol *p*-nitrophenol per min under assay conditions.[18] Proteins from soluble and insoluble fractions were also analyzed by separating (12%) and stacking (4%) SDS polyacrylamide gels.[25] After electrophoresis the gels were first activity stained with α-naphthylacetate and Fast Red[18] followed by Coomassie brilliant blue staining.

Creation of epPCR library: Plasmids, isolated with the QIAprep kit (Qiagen, Hilden, Germany) were used in epPCR experiments at a final concentration of 0.1 ng μL^{-1}. The reaction mixture consisted of dNTP Mix (10 μL; 2 mM ATP, 2 mM GTP, 10 mM CTP, 10 mM TTP), mutation buffer (10 μL; 70 mM $MgCl_2$, 500 mM KCl, 100 mM Tris pH 8; 0.1% (*w*/*v*) gelatine), primers (100 pmol of each; forward primer: GACTGGTCGTAATGAACAATTC; reverse primer: AATGATGATGATGATGGCATC), *Taq* polymerase (1 μL, 5 U μL^{-1}), $MnCl_2$ (3 μL, 10 mM) and plasmid DNA in a final volume of 100 μL. The reaction conditions were: 1) 95 °C 60 s, 2) 25 cycles: 95 °C 30 s, 50 °C 30 s, 72 °C 45 s, 3) 72 °C 150 s. PCR products were purified with the QIAquick™ PCR Purification Kit, digested with *Bam*HI and *Nde*I to generate cohesive ends, ligated in the empty vector pJOE2792.1 and transformed into competent *E. coli* cells that had been prepared by using the rubidium chloride method. Transformants were transferred by replica plating to LB/Amp (100 μg) agar plates containing L-rhamnose (final concentration 0.2% *v*/*v*) to induce esterase production and to enable the activity towards α-naphthylacetate to be analysed. Active clones showing a red colour with Fast Red were transferred to microtiter plates (MTPs) containing LB/Amp (200 μL) in each well (master plate). The plates were incubated for 16 h at 37 °C and 50 rpm, glycerol or DMSO (end concentration 10%, *v*/*v*) were added and the MTP was stored at −80 °C.

Enzyme production in MTPs with "steady-state growth method": Master plates were duplicated by transferring colonies with a 96 pin head onto a new MTP containing LB/Amp (200 μL per well; production plate). These new plates were incubated for 24 h at 37 °C and 50 rpm; the cultures were then at the stationary growth phase. A sample of the culture (100 μL) was transferred with a pipet robot (Miniprep 75, Tecan, Crailsheim, Germany) from each well to a new MTP well containing fresh LB/Amp (100 μL) and incubated for a further 3 h to reach the exponential phase. Next, L-rhamnose was added to induce esterase production for another 5 h. Cells were harvested by centrifugation (1750 g, 15 min, 4 °C) and supernatants were discarded. Lysis buffer (200 μL; 300 mM NaCl, 50 mM Na_2HPO_4, pH 8) containing DNAseI (final concentration 1 U mL^{-1}) and lysozyme (final concentration 0.1%, *w*/*v*) were added and cells were destroyed by one freeze-thaw-cycle. The supernatant containing the esterase was either lyophilized or directly stored at −20 °C. As the soluble protein contained mostly the recombinant esterase (about 50% of total protein), the crude lyophilisate was not purified before the activity and kinetic data were determined.

Synthesis of corresponding racemic and enantiopure acetates: Acetates were enzymatically synthesized in a transesterification reaction from *rac*-**1a** (1 equiv) with vinyl acetate (1.5 equiv) in *n*-hexane (5 mL). Reaction mixtures contained molecular sieves and *Candida antarctica* lipase B (5 mg; CAL-B, Novozym, Denmark) and were stirred at 37 °C, overnight. Enzyme and molecular sieves were removed by centrifugation, solvent and excess vinyl acetate were evaporated. As CAL-B exhibited no enantioselectivity towards **1a**, complete conversion to the racemic acetate was possible.

Screening with the acetic acid assay: The test kit for the determination of released acetic acid was from R-Biopharm GmbH (Darmstadt, Germany) and applied according to the manufacture's protocol. Enzyme solution (20 μL) from the production plate and substrate solution (20 μL; 7.5 mg mL^{-1}) of enantiopure (*R*)- or (*S*)-2-acetoxybut-3-yn (**1b**) were added to a mixture (150 μL) of the test kit components. The increase of NADH was monitored at 340 nm by

using the Fluostar Galaxy or Fluostar Optima (BMG, Offenburg, Germany). Mixtures of test kit components with buffer or cell lysate from induced *E. coli* that contained a vector without an esterase gene, served as controls. The ratio of the initial rates thus determined for each enantiomer was defined as the apparent enantioselectivity (E_{app}).[17]

General method for esterase-catalyzed small-scale resolutions: Esterase solution was added to a stirred solution of substrate **1b** (25 mM) in phosphate buffer (10 mM, pH 7.4). The reaction mixture was stirred in a thermoshaker (Eppendorf, Hamburg, Germany) at 37 °C. At different time points, samples (100 μL) were taken and extracted twice with dichloromethane (100 μL). The combined organic layers were dried over anhydrous sodium sulphate and the organic solvent was removed under nitrogen. The samples were analyzed by gas chromatography (GC-14A gas chromatograph, Shimadzu, Japan) by using a chiral column Hydrodex®-β-3P (heptakis-(2,6-di-*O*-methyl-3-*O*-pentyl)-β-cyclodextrin; 0.25 mm) with hydrogen as carrier gas. Enantioselectivity (E_{true}) and conversion were calculated according to Chen et al.[26]

QuikChange: The QuikChange™ Site-Directed Mutagenesis Kit (Stratagene, La Jolla, USA) was used according to the manufacturer's instructions with complementary primers: G229A exchange: 5′-CTTCGCCGACGACATCGCCCAGTTGATC-3′, C296G exchange: 5′-CATGGGCGGCGGCGATGTGGCCCG-3′ and C527T exchange: 5′-TCTCCCAAGGCGTGCAGACCCAGACC-3′. The plasmid encoding for the triple mutant (0.1 ng μL^{-1} as template) and the following reaction conditions: 1) 95 °C 45 s, 2) 20 cycles: 95 °C 45 s, 55 °C 60 s, 68 °C 10 min. The mutated plasmids were transformed into competent *E. coli* cells (4 μL reaction in 50 μL competent cells).

Molecular-dynamic simulation: The effect of mutations on the structure of the PFE enzyme was investigated by a molecular-dynamics simulation according to the following procedure. One chain of the hexamer (PBD ID: 1VA4) was used as model for the wild-type PFE and a mutant containing three mutations (Ile76Val, Gly98Ala, Val175Ala) was generated from this strand. Both proteins were embedded into orthorombic cells containing around 9000 water molecules that provided a layer of at least 10 Å in thickness. The AMBER94 forcefield as implemented in the AMBER7 package was used including the TIP3P model for water. Geometry optimization was performed in three stages (12000 steps each) which provided the optimization of the water and protein molecule alone and of the total system. A molecular dynamics run of 20000 steps corresponding to 20 ps at constant pressure and temperature (NpT) resulted in a slight reduction of the cell size to $68.77 \times 64.32 \times 68.83$ Å^3, thus attaining a standard water density. After this relaxation a production run of 200 ps without temperature and pressure control (NVE) was added.

The alignment of the resulting structures for wild-type and mutant enzymes was performed with PyMOL (http://pymol.sourceforge.net).

Acknowledgements

Financial support by the Deutsche Bundesstiftung Umwelt (Osnabrück, Germany, grant no. AZ13062) is gratefully acknowledged.

Keywords: directed evolution · enantioselectivity · enzyme catalysis · esterases · protein engineering

[1] a) H. F. Arnold, A. A. Volkov, *Curr. Opin. Chem. Biol.* **1999**, *3*, 54–59; b) U. T. Bornscheuer, *Angew. Chem.* **1998**, *110*, 3285–3288; *Angew. Chem. Int. Ed.* **1998**, *37*, 3105–3108; c) K.-E. Jaeger, T. Eggert, *Curr. Opin. Biotechnol.* **2004**, *15*, 305–513; d) M. T. Reetz, *Proc. Natl. Acad. Sci. USA* **2004**, *101*, 5716–5722.
[2] O. May, P. T. Nguyen, F. H. Arnold, *Nat. Biotechnol.* **2000**, *18*, 317–320.
[3] M. T. Reetz, A. Zonta, K. Schimossek, K. Liebeton, K.-E. Jaeger, *Angew. Chem.* **1997**, *109*, 2961–2963; *Angew. Chem. Int. Ed. Engl.* **1997**, *36*, 2830–2832.
[4] a) K. Liebeton, A. Zonta, K. Schimossek, M. Nardini, D. Lang, B. W. Dijkstra, M. T. Reetz, K.-E. Jaeger, *Chem. Biol.* **2000**, *7*, 709–718; b) M. T. Reetz, *Tetrahedron* **2002**, *58*, 6595–6602.
[5] E. Henke, U. T. Bornscheuer, *Biol. Chem.* **1999**, *380*, 1029–1033.
[6] K. L. Morley, R. J. Kazlauskas, *Trends Biotechnol.* **2005**, *23*, 231–237.
[7] R. J. Kazlauskas, A. N. E. Weissfloch, A. T. Rappaport, L. A. Cuccia, *J. Org. Chem.* **1991**, *56*, 2656–2665.
[8] W. P. Gallagher, R. E. J. Maleczka, *J. Org. Chem.* **2003**, *68*, 6775–6779.
[9] H. Ko, E. Kim, J. E. Park, D. Kim, S. Kim, *J. Org. Chem.* **2004**, *69*, 112–121.
[10] G. A. Molander, J. P. Burke, P. J. Carroll, *J. Org. Chem.* **2004**, *69*, 8062–8069.
[11] X. Fu, J. Yin, Thiruvengadam, K. T. McAllister, L. T. C.-H. Tann, C. Colon, *Org. Process Res. Dev.* **2002**, *6*, 308–310.
[12] J. Pietruszka, N. Schöne, *Eur. J. Org. Chem.* **2004**, *24*, 5011–5019.
[13] A. Horváth, J. Benner, J. E. Baeckvall, *Eur. J. Org. Chem.* **2004**, *15*, 3240–3243.
[14] R. Yanada, Y. Koh, N. Nishimori, A. Matsumura, S. Obika, H. Mitsuya, N. Fujii, Y. Takemoto, *J. Org. Chem.* **2004**, *69*, 2417–2422.
[15] F. W. Hartner, Y. Hsiao, K. K. Eng, N. R. Rivera, M. Palucki, L. Tan, N. Yasuda, D. L. Hughes, S. Weismann, D. Zewge, T. King, D. Tschaen, R. P. Voante, *J. Org. Chem.* **2004**, *69*, 8723–8730.
[16] M. Yoshida, Y. Ohsawa, M. Ihara, *J. Org. Chem.* **2004**, *69*, 1590–1597.
[17] M. Baumann, B. H. Hauer, U. T. Bornscheuer, *Tetrahedron Asymmetry* **2000**, *11*, 4781–4790.
[18] N. Krebsfänger, F. Zocher, J. Altenbuchner, U. T. Bornscheuer, *Enzyme Microb. Technol.* **1998**, *22*, 641–646.
[19] B. Hauer, T. Friedrich, C. Nübling, R. Stürmer, **2002**. German patent application, DE10042892A1, 31.08.2000.
[20] K. Nakamura, K. Takenaka, *Tetrahedron Asymmetry* **2002**, *13*, 415–422.
[21] T. Schubert, W. Hummel, M. R. Kula, M. Müller, *Eur. J. Org. Chem.* **2001**, *22*, 4181–4187.
[22] M. Baumann, R. Stürmer, U. T. Bornscheuer, *Angew. Chem.* **2001**, *113*, 4329–4333; *Angew. Chem. Int. Ed.* **2001**, *40*, 4201–4204.
[23] J. D. Cheeseman, A. Tocilj, S. Park, J. D. Schrag, R. J. Kazlauskas, *Acta Crystallogr. Sect. D Biol. Crystallogr.* **2004**, *60*, 1237–1243.
[24] P. Y. Chou, G. D. Fasman, *Biochemistry* **1974**, *13*, 211–222.
[25] J. Sambrook, E. F. Fritsch, T. Maniatis, *Molecular Cloning: A Laboratory Manual*, 2nd ed., Cold Spring Harbor Laboratory Press, New York, **1989**.
[26] C. S. Chen, Y. Fujimoto, C. J. Sih, *J. Am. Chem. Soc.* **1982**, *104*, 7294–7299.

Received: December 19, 2005
Published online on March 31, 2006

